Arch Neurosci. 2015 October; 2(4): e27768. DOI: 10.5812/archneurosci.27768
Published online 2015 October 24. **Research Article**

Demonstration of Differentially Degenerated Corpus Callosam in Patients With Moderate Traumatic Brain Injury: With a Premise of Cortical-callosal Relationship

Kavita Singh,[1] Richa Trivedi,[1,*] Maria M. D'souza,[1] Ajay Chaudhary,[2] Subash Khushu,[1] Pawan Kumar,[1] Ram K. S. Rathore,[3] and Rajendra P. Tripathi[2]

[1]NMR Research Centre, Institute of Nuclear Medicine and Allied Sciences, Delhi, India
[2]Department of Neurosurgery, Dr. Ram Manohar Lohia Hospital, Delhi, India
[3]Department of Mathematics, Indian Institute of Technology, Kanpur, UP, India

*Corresponding author: Richa Trivedi, NMR Research Centre, Institute of Nuclear Medicine and Allied Sciences, Delhi, India. Tel: +91-01123905369, Fax: +91-01123919509, E-mail: triricha@gmail.com

Received: February 20, 2015; **Accepted:** February 24, 2015

Background: Traumatic brain injury (TBI) has been shown to predominantly affect the corpus callosum (CC). In light of the anatomical organization of cortico-callosal connections, we hypothesized that injury to the different cortical lobes may specifically affect their corresponding subdivisional fibers in the CC.
Objectives: The aim of this study was to investigate lesion-related Wallerian degeneration across the subdivisions of the CC in patients with moderate TBI.
Patients and Methods: Diffusion tensor tractography (DTT) was performed between 14 days and 6 months after trauma in 18 patients with moderate TBI, and 11 age- and gender-matched healthy control subjects. Based on conventional magnetic resonance imaging findings, patients were classified into 3 groups: A) frontal lobe injury; B) occipito-temporal lobe injury; and C) fronto-parieto-temporal lobe injury. The CC was divided into seven subdivisions based on Witelson's classifications. Fractional anisotropy (FA) and mean diffusivity (MD) values from the seven segments were compared among patient groups and controls.
Results: Compared to controls, Group A showed significantly reduced FA in the rostrum, genu, splenium, and CC. Group B showed significantly reduced FA in the isthmus and whole CC relative to that in the controls. In Group C, FA significantly decreased across the entire CC compared to that in the controls.
Conclusions: In our study, subdivisional fibers of the CC showed secondary microstructural changes resulting from primary injury in the corresponding cortical areas. We conclude that DTT-derived measures may act as an indicator of ongoing Wallerian degeneration. By extension, this study may improve our understanding of variable neuropsychological outcomes in clinically similar patients with TBI.

Keywords: Brain Injuries; Wallerian Degeneration; Corpus Callosum; Diffusion Tensor Imaging; Fractional Anisotropy

1. Background

Traumatic brain injury (TBI) has been defined as altered brain function or pathology caused by an external mechanical force (1). It is a leading cause of mortality and morbidity, and there are no effective therapies that reduce mortality rates or limit disability following injury (2). Thus, TBI does not merely involve a single event, but rather an ongoing pathophysiological process comprising primary and secondary mechanisms of injury that together lead to structural damage and functional deficits. Associated neuropsychological deficits include memory, executive function, and attentional impairment; behavioral and personality changes; and slowed information processing (3-5). The primary injury which is the direct result of external force, involves tissue deformation leading to secondary injury. Inflammation, apoptosis, and diffuse axonal injury (DAI) are reported to be among the important cellular processes underlying secondary injury (6).

Trauma-induced white matter (WM) damage from DAI has been shown to disrupt brain connectivity (7). Focal lesions in TBI can be easily identified using conventional imaging. However, DAI is not readily observed. Consequently, advanced diffusion tensor imaging (DTI) technology has been utilized to study DAI following TBI (8, 9). DTI is based on the assumption that directionality and diffusivity of constantly moving water molecules are indicative of the integrity of neural structures (10). Major WM fibers of interest can be 3-dimensionally re-

constructed using diffusion tensor tractography (DTT) and visualized to identify putative changes in connectivity that cannot be seen on conventional MRI (11). Altered pathology can be inferred from DTI metrics, e.g. fractional anisotropy (FA) and mean diffusivity (MD). FA indicates the degree of directionality or axon alignment, while MD represents the degree of restriction of movement of water molecules through cells located within a fiber sample (12).

Various DTI studies of TBI have shown that there are altered diffusivities in the corpus callosum (CC), anterior limb of the internal capsule, cingulum bundles, uncinate fasciculus, centrum semiovale, thalamic WM projections, and inferior and superior longitudinal fascicules. CC has been shown to be among the most affected structures (13) depending on the amount of time after injury, severity, and subject age (9, 14-21). Callosal damage has also been observed in children and adolescents with TBI (22, 23).

The CC, which contains approximately 200 to 800 million axons, is the largest and most dense commissural fiber tract (24), and it is the tract most vulnerable to rotational acceleration and deceleration following TBI. TBI-related axonal injury in the CC has been reported to result from high shear strain forces generated by the long coursing structure of the CC and its midline location adjacent to the flax cerebri.

Based on Witelson's classifications, the CC has been divided into 7 segments: rostrum, genu, rostral body (RB), anterior mid body (AMB), posterior mid body (PMB), splenium, and isthmus (25). Studies have shown that deviant asymmetry of cortical areas of the brain may be related to the callosal abnormalities present in developmental dsylexia (26). In addition, studies of individuals with autism have shown that there are abnormalities in subregions of the corpus callosum that correlate with functional deficits in the corresponding cortical lobes (27). Specifically, it was shown that functional deficits in functions controlled by the frontal lobe, such as executive functions, complex language skills, and reasoning, were mainly attributable to structural abnormalities in the subregions of the CC that were connected to the corresponding lobe (27).

Studies using advanced neuroimaging techniques to characterize TBI pathology have shown wide variations in their results and conclusions (28-30). In a study of moderate to severe chronic TBI (31), a significant correlation between atrophy of the CC and reaction time (a behavioral measure) was not observed. Heterogeneity in the deficits that result from TBI may be attributed to the location, nature, and severity of primary injury, as well as pre-existing conditions and demographic characteristics (e.g. age, sex, substance abuse, and genetic differences) (32). Although studies have shown that the degree of CC involvement in TBI depends on the severity of injury, to our knowledge, no study has yet determined if there is a correlation between injuries to specific regions of the cortex and abnormalities in the corresponding subdivisonal fibers of the CC.

2. Objectives

Based on the established cortico-callosal connections and studies of persistent cognitive impairment and continued WM degeneracy in post TBI patients, we hypothesized that extent of damage to a subdivision of CC due to TBI is in a way related to the corresponding cortical area primarily injured. To verify this hypothesis, we divided patients with moderate TBI into three groups based on the cortical region that contained the primary site of injury.

3. Patients and Methods

3.1. Participants: Demographics and Clinical Details

18 patients with moderate TBI (right handed, 13 males and 5 females; 25.3 ± 9.1 years [mean ± SD]; range = 16 - 45 years) and 11 neurologically healthy control subjects matched for age, gender, and education (right handed, 6 males and 5 females; 27.6 ± 8.3 years [mean ± SD]; range 18 - 43 years) were included in this study. Demographic and clinical characteristics for both groups are given in Table 1. The patients were included based on the following criteria: 1) moderate cortical head injury; 2) absence of signal abnormalities in the CC on T2-weighted, FLAIR, and SWI images; 3) no use of any medication during the study period. The severity of TBI was assessed based on the Glasgow Coma Scale (33): GCS score 9 - 12. DTI scans were performed between 14 days to 6 months (4.13 ± 1.87 months [mean ± SD]) of the initial traumatic insult. Potential subjects in the control and patient groups with a history of head trauma, substance abuse, and other neurological or psychiatric illnesses were excluded. Each participant in the study signed an informed consent form. The institutional ethics and research committee approved this study.

3.2. Image Acquisition

Imaging was performed using a 3-Tesla MRI scanner (Megnetom, Skyra, Siemens) with a 25 mT/m actively shielded gradient system and a 20-channel head coil. Subjects were instructed to remain still during the acquisition to minimize the effect of movement. The head was supported and immobilized within the head coil and foam padding was kept around the ears to reduce gradient noise. Conventional MR imaging was conducted in addition to DTI to detect the lesion site (Figure 1). The imaging parameters for T2-weighted fast spin echo sequence were: repetition time /echo time/ number of excitations (TR)/(TE)/(NEX) = 5600 ms/100 ms/2). T1-weighted spin echo (SE) was obtained using:

TR = 2000 ms, TE = 859 ms, NEX = 1; while the T2-fluid attenuated inversion recovery (FLAIR) sequence was obtained using: TR = 9000 ms, TE = 81 ms, inversion time = 2500 ms, NEX = 1. Susceptibility weighted imaging was conducted using the following parameters: TR = 28 ms, TE = 20 ms, NEX = 1, slice thickness = 1.5 mm, flip angle = 15°, FoV = 220 × 192.

DTI images were acquired in 30 directions using a single-shot, echo-planar dual SE sequence with ramp sampling; b-factors of 0 and 1000 s/mm^2 were used for acquisition with a slice thickness of 3 mm and no inter-slice gap. A total of 45 slices were acquired with an FOV of 230 mm × 230 mm. The imaging matrix size was 128 × 128; other parameters were: a flip angle of 90°, TR = 8800 ms, TE = 95 ms, and NEX = 2.

3.3. Segmentation of White Matter Structures and Diffusion Tensor Tractography

White matter segmentation was done as described in detail elsewhere (34). In addition, the segmented components were reconstructed and fiber assignment was carried out with a continuous tracking algorithm to generate the fiber bundles of interest (35). Specific WM fiber bundles and their related anatomy were identified in these reconstructions, and various DTI measures were calculated for the desired WM fiber bundles. Fibers with FA values more than 0.15 were considered for tractography.

An ROI in the mid-sagittal slice was selected for generating CC tracts, and was then further subdivided into seven sub divisions based on Witelson's classifications (25): rostrum, genu, rostral body (RB), anterior mid body (AMB), posterior mid body (PMB), isthmus, and splenium, which approximately represent the CC connections that are hypothesized to distinguish callosal connections from distinct cortical brain regions (25). For all subdivisions of the CC and the CC as a whole, fibers were successfully generated and DTI measures were quantified (Figure 2 A).

3.4. Statistical Analysis

One-way analysis of variance (ANOVA) with post-hoc and Bonferroni corrections was performed to study the difference in DTI measures among patient groups and controls. P values of less than 0.05 were considered to be statistically significant. Data were analyzed using SPSS (version 16.0, SPSS Inc. Chicago, IL, USA).

4. Results

Among the 18 patients with TBI, six had frontal lobe injury (n = 6), five had occipito-temporal lobe injury (n = 5), and seven had fronto-parieto-temporal lobe injury (n = 7). None of these patients exhibited CC injury on conventional imaging. Based on these conventional imaging findings, patients were classified into three groups: frontal lobe injury patients (Group A); occipito-temporal lobe injury patients (Group B); and fronto-parieto-temporal lobe injury patients (Group C) (Figure 2 B).

4.1. Quantitative Analysis

The TBI group did not show any significant differences from control subjects in age, education, or handedness. The FA and MD values (mean ± SD) collected from the various subdivisions of the CC from patients and controls are listed in Tables 2 and 3, respectively.

4.2. Group A versus Control

Compared to the control group, Group A exhibited significantly decreased FA values in the rostrum, genu, splenium, and CC as a whole. MD values in the rostrum and genu significantly increased in Group A compared to the values in the controls, while increases in MD values in the splenium did not reach the level of statistical significance.

Table 1. Demographic Data and Clinical Details of the TBI and Control Groups [a,b]

Demographics	TBI (N = 18)	Control (N = 11)	P Value
Gender (male/female)	13/5	6/5	ns
Age, y	25.3 ± 9.1	27.6 ± 8.3	ns
GCS	9 - 12	--	
Time since injury, months	4.13 ± 1.87	--	

[a] Abbreviation: ns, non-significant.
[b] Values are presented as mean ± SD.

Figure 1. Example of an Age Matched Control

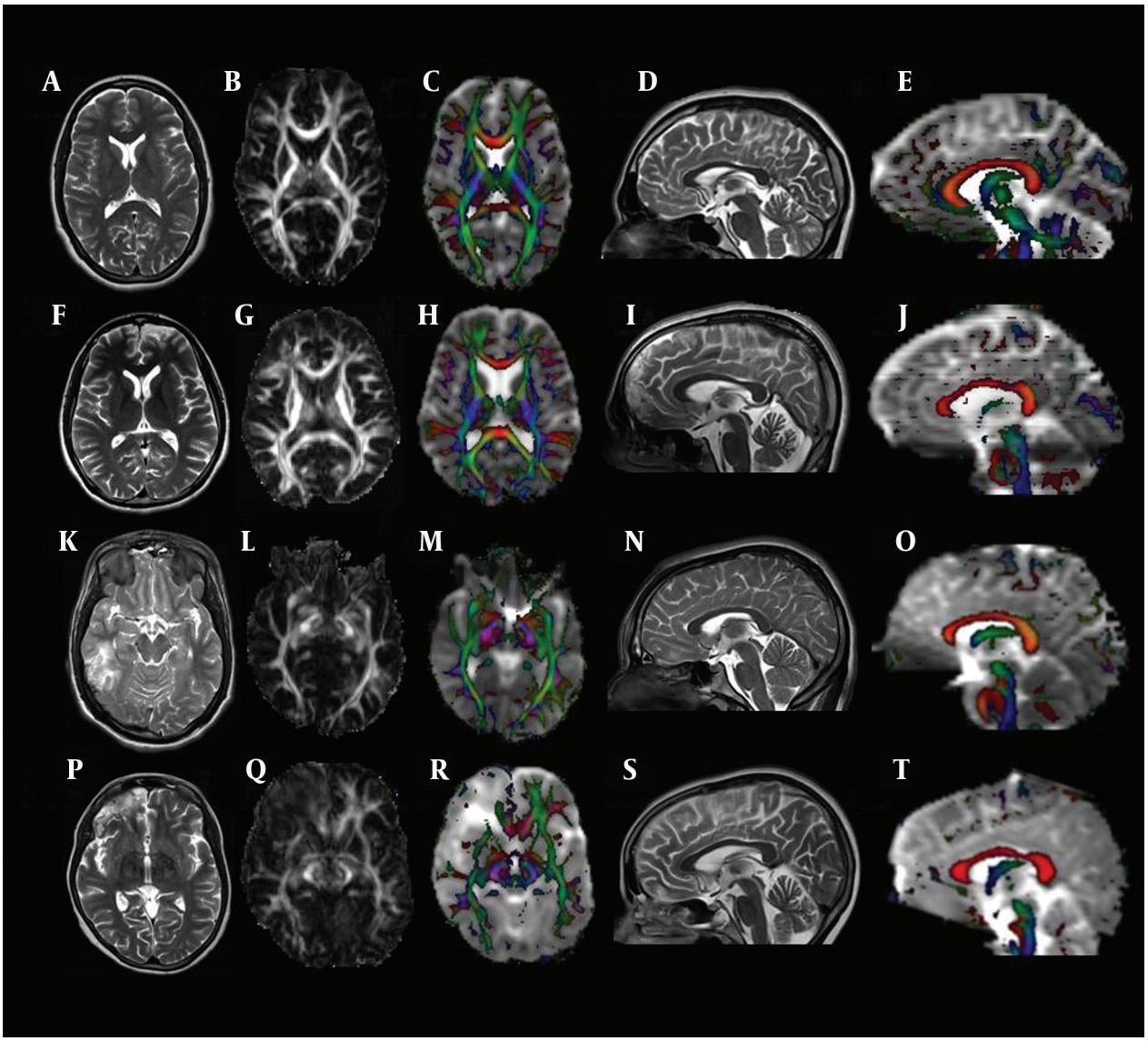

Figure showing the normal distribution of gray and white matter on T2-weighted images of the brain parenchyma (a), an FA map (b), a color coded FA map overlaid on MD (c), mid-sagittal T2-weighted (d) images, and a mid-sagittal color coded FA map overlaid on MD (e). Axial T2-weighted images from patients in Group A (f-j), Group B (k-o), and Group C (p-t) showing hyperintense lesions in the left frontal region (f), right temporal region (k), and right fronto-temporal region (p), respectively. A decrease in FA values is evident in all three patient groups on the corresponding axial FA (g, l, q) and a color-coded FA map overlaid on MD (h, m, r). The corpus callosum (CC) appears normal in a mid-sagittal T2-weighted image of all three groups (i, n, s); however, the sagittal color-coded FA map (j, o, t) shows decreased FA values in the CC in all three patient groups.

4.3. Group B versus Control

Group B patients showed decreased FA values in fibers of the PMB, isthmus, splenium, and CC as a whole compared to those shown by control participants. However, a significant difference was observed in the isthmus and CC as a whole. Increased MD values were observed in fibers of the isthmus, splenium, and CC as a whole compared to those in the controls.

4.4. Group C versus Control

FA values significantly decreased in Group C compared to those in the controls in fibers of all subdivisions and the CC as a whole. MD values showed significant increases in the genu, splenium, and CC as a whole in Group C compared to those in the controls. Other subdivisions showed modest increases in Group C compared to those in the controls.

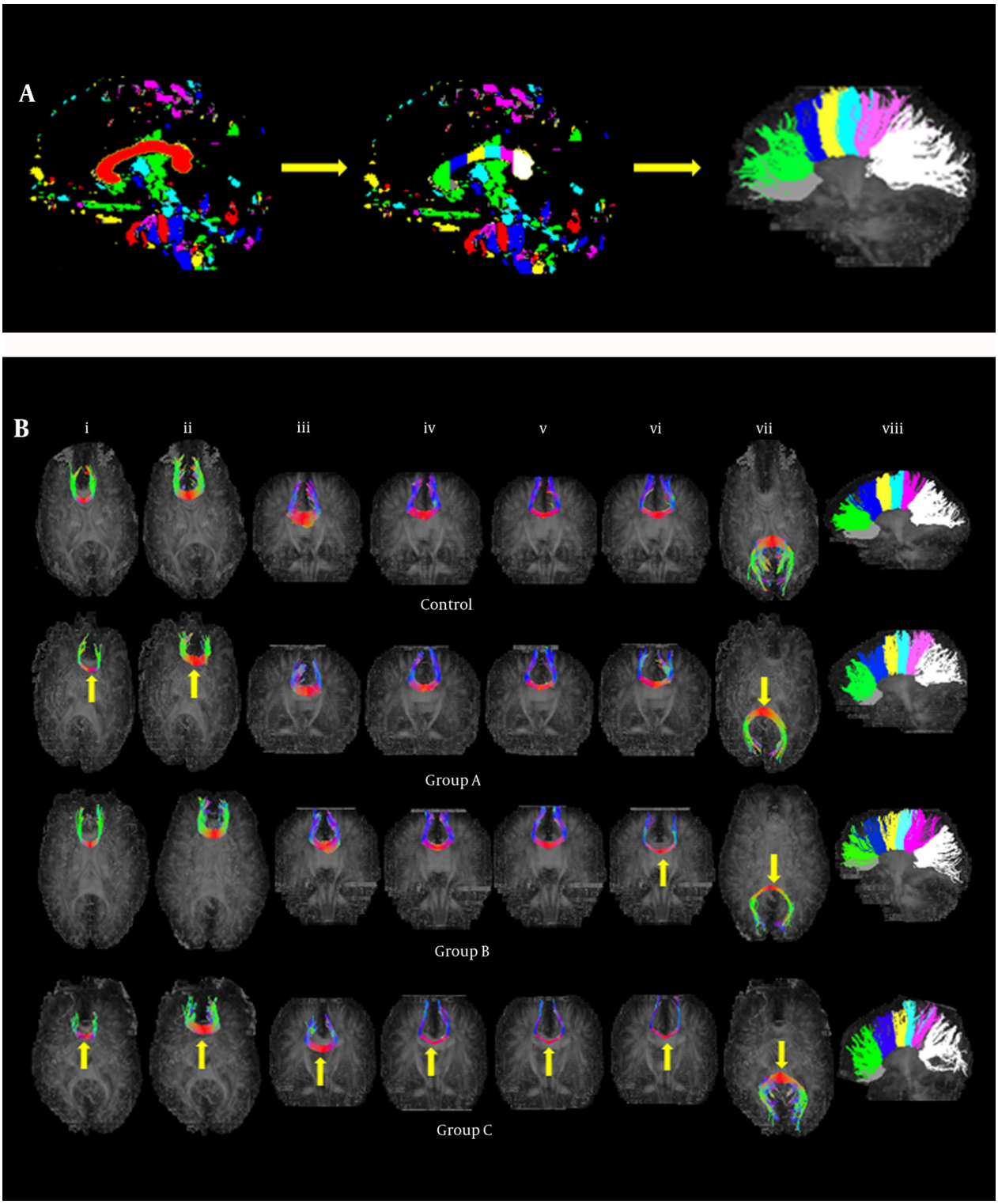

Figure 2. A, The methodology used for reconstruction and segmentation of the corpus callosum (CC) into seven subdivisions (rostrum: grey, genu: green, rostral body: blue, anterior mid-body: yellow, posterior mid-body: turquoise, isthmus: pink, splenium: white) based on Witelson's classifications applied to a healthy participant. B, Reconstructed subdivisional callosal fibers in the control group, Group A, Group B, and Group C. In Group A, thinning of the CC (yellow arrow) is apparent in the rostrum, genu, and splenium compared to that in the control group. Group B exhibited thinning of the CC in both the isthmus and splenium compared to that in the control group. In Group C, all CC subdivisions were thinner than in the control group.

Table 2. The FA values (Mean ± SD) for Various Subdivisions of the CC from the Control Group and Patients Groups A, B, and C [a]

Fiber Bundle	Control[0]	Group A[A]	Group B[B]	Group C[C]	Statistical Significance (P Value) Difference on Bonferroni Post-Hoc Test
Rostrum	0.42 ± 0.03	0.34 ± 0.05 [b]	0.41 ± 0.04	0.36 ± 0.05 [b]	p_{0A} (0.01), p_{0B} (1.00), p_{0C} (0.04), p_{AB} (0.11), p_{AC} (1.00), p_{BC} (0.39)
Genu	0.49 ± 0.02	0.43 ± 0.03 [b]	0.46 ± 0.02	0.43 ± 0.04 [b]	p_{0A} (0.01), p_{0B} (0.87), p_{0C} (0.01), p_{AB} (0.50), p_{AC} (1.00), p_{BC} (0.20)
Rostral body	0.46 ± 0.02	0.44 ± 0.04	0.44 ± 0.04	0.41 ± 0.03 [b]	p_{0A} (0.81), p_{0B} (0.67), p_{0C} (0.01), p_{AB} (1.00), p_{AC} (0.31), p_{BC} (0.53)
AMB	0.50 ± 0.02	0.48 ± 0.03	0.47 ± 0.03	0.44 ± 0.03 [b]	p_{0A} (0.54), p_{0B} (1.00), p_{0C} (0.01), p_{AB} (1.00), p_{AC} (0.05), p_{BC} (0.42)
PMB	0.51 ± 0.02	0.48 ± 0.04	0.47 ± 0.01	0.44 ± 0.03 [b]	p_{0A} (0.50), p_{0B} (0.06), p_{0C} (0.01), p_{AB} (1.00), p_{AC} (0.06), p_{BC} (0.70)
Isthmus	0.48 ± 0.02	0.45 ± 0.01	0.42 ± 0.05 [b]	0.41 ± 0.03 [b]	p_{0A} (0.24), p_{0B} (0.01), p_{0C} (0.01), p_{AB} (1.00), p_{AC} (0.20), p_{BC} (1.00)
Splenium	0.52 ± 0.02	0.48 ± 0.01 [b]	0.49 ± 0.02	0.46 ± 0.03 [b]	p_{0A} (0.03), p_{0B} (0.06), p_{0C} (0.01), p_{AB} (1.00), p_{AC} (0.60), p_{BC} (0.60)
CC	0.50 ± 0.02	0.46 ± 0.02 [b]	0.46 ± 0.02 [b]	0.44 ± 0.02 [b]	p_{0A} (0.01), p_{0B} (0.03), p_{0C} (0.01), p_{AB} (1.00), p_{AC} (0.21), p_{BC} (0.18)

[a] Abbreviations: AMB, anterior mid body; CC, corpus callosum; PMB, posterior mid body; P0A, denotes P value of control versus group A; p0B, denotes P value of control versus group B; p0C, denotes P value of control versus group C; pAB, denotes P value of group A versus group B; pAC, denotes P value of group A versus group C; pBC, denotes P value of group B versus group C.
[b] Denotes P value ≤ 0.05.

Table 3. MD Values (Mean ± SD) for Various Subdivisions of the CC from the Control Group and Patient Groups A, B, and C [a]

Fiber Bundle	Control[0]	Group A[A]	Group B[B]	Group C[C]	Statistical significance (P Value) Difference on Bonferroni Post-Hoc Test
Rostrum	0.95 ± 0.07	1.14 ± 0.14 [b]	0.99 ± 0.08	1.08 ± 0.12	p_{0A} (0.01), p_{0B} (1.00), p_{0C} (0.07), p_{AB} (1.00), p_{AC} (1.00), p_{BC} (0.74)
Genu	0.87 ± 0.04	0.98 ± 0.12 [b]	0.92 ± 0.06	0.99 ± 0.08 [b]	p_{0A} (0.04), p_{0B} (1.00), p_{0C} (0.02), p_{AB} (1.00), p_{AC} (1.00), p_{BC} (0.64)
Rostral body	0.88 ± 0.06	0.93 ± 0.10	0.93 ± 0.12	0.98 ± 0.07	p_{0A} (1.00), p_{0B} (1.00), p_{0C} (0.11), p_{AB} (1.00), p_{AC} (1.00), p_{BC} (1.00)
AMB	0.86 ± 0.04	0.87 ± 0.06	0.89 ± 0.08	0.94 ± 0.07	p_{0A} (1.00), p_{0B} (1.00), p_{0C} (0.14), p_{AB} (1.00), p_{AC} (0.30), p_{BC} (1.00)
PMB	0.88 ± 0.04	0.88 ± 0.07	0.90 ± 0.06	0.95 ± 0.08	p_{0A} (1.00), p_{0B} (1.00), p_{0C} (0.10), p_{AB} (1.00), p_{AC} (0.33), p_{BC} (1.00)
Isthmus	0.96 ± 0.06	1.00 ± 0.05	1.05 ± 0.10	1.03 ± 0.09	p_{0A} (1.00), p_{0B} (0.15), p_{0C} (0.36), p_{AB} (1.00), p_{AC} (1.00), p_{BC} (1.00)
Splenium	0.92 ± 0.04	0.98 ± 0.04	1.01 ± 0.05 [b]	1.01 ± 0.05 [b]	p_{0A} (0.11), p_{0B} (0.01), p_{0C} (0.01), p_{AB} (0.85), p_{AC} (1.00), p_{BC} (1.00)
CC	0.91 ± 0.04	0.95 ± 0.06	0.97 ± 00.06	0.99 ± 0.05 [b]	p_{0A} (0.35), p_{0B} (0.18), p_{0C} (0.01), p_{AB} (1.00), p_{AC} (1.00), p_{BC} (1.00)

[a] AMB, anterior mid body; CC, corpus callosum; PMB, posterior mid body; P0A, denotes P value of control versus group A; p0B, denotes P value of control versus group B; p0C, denotes P value of control versus group C; pAB, denotes P value of group A versus group B; pAC, denotes P value of group A versus group C; pBC, denotes P value of group B versus group C.
[b] Denotes P value ≤ 0.05.

5. Discussion

Here, we demonstrate the degenerative changes, secondary to TBI, in the sub divisional fibres of CC which showed a direct association to the corresponding cortical lobes primarily involved in injury. Compared to the controls, patients with moderate TBI (based on GCS Score) showed microstructural damage to the CC during subacute to chronic phases of insult when no damage was visible on conventional MRI.

A study (36) of 42 closed head injury patients in a post-traumatic persistent vegetative state showed DAI in the CC in all cases. Additional studies (16) have shown WM loss between 2 to 12.7 months post TBI that was particular-

ly prominent in the CC. Trauma-induced atrophy of the CC may be due to either direct effects of trauma to the CC itself (37, 38) or Wallerian-type secondary degeneration (WD) resulting from diffuse brain damage that disrupts the integrity of white matter fibers (39). WD has been defined as a spontaneous process involving degeneration of axons that have been separated from their respective cell bodies (40). WD in humans initiates as early as 1 - 2 hours post-injury (41) and can last for several months (42). During WD, axons distal to the injury site undergo cytoskeletal disassembly and granular degeneration (43, 44). This is followed by blood-brain barrier breakdown and removal of axonal and myelin debris by local and infiltrating reactive glial cells.

The pathological process in WD has been characterized using conventional MR (45). Changes from 20 days to 2 - 4 months appear as a low signal on T2 images, as tracts become hydrophobic due to myelin and protein breakdown. This hydrophobicity leads to accumulation of water in the oedematous demyelinating tracts which is subsequently visible as increased signal intensity on MRI. A correlation of the long-term clinical outcome in WD with the early changes in diffusion indices in the cortico-spinal tract (CST) of post-stroke patients has been reported (46). This study showed monotonously decreased anisotropy and increased diffusivity (though this was stable during the first 2 weeks after injury) of the degenerated CST during the first 3 months (though they were stable during the first 2 weeks after injury), which then remained relatively unchanged. A study (47) on individuals with focal infarcts that exhibited water diffusion changes associated with WD showed that diffusivity is greatly increased in the primary lesion, but only slightly increased in areas undergoing WD. This has been explained on the basis that in regions primarily affected by stroke, there is formation of CSF filled cystic spaces in regions primarily affected by stroke. The increased content of unhindered, isotropically diffusing water in these cavities led to discernible increases in diffusivity. Moreover, there was an overall increase of diffusivity at the site of the primary lesion. By contrast, WD showed a limited increase in diffusivity as there was neither formation of cysts nor significant water accumulation in the interstitial space. Studies have demonstrated WD in CC in brain tumors patients where tumors do not infiltrate the CC (48). Another imaging study of temporal lobe epilepsy showed changes not only in the seizure site, but also in remote locations such as the splenium of CC owing to secondary WD-mediated white matter degeneration (49). In view of the above studies, our findings of altered DTI measures (decreased FA and increased MD) in patients with moderate TBI may be due to WD.

de Lacoste et al. (51) reported a relationship between cortical lesion sites in ischemic infarctions or circumscribed contusions and WD in the corresponding regions of the CC in 13 postmortem brains. Cortico-callosal connections and the topography of the callosal fibers in relation to their cortical regions of origin and termination have been studied widely in primates (50) and human clinical studies (51). Witelson measured the whole CC in 50 human post-mortem brains and subsequently divided it into 7 subdivisions (25). In the present study, we have segmented the CC based on Witelson's classifications, in which the rostrum contains fibers from the caudal/orbital prefrontal and inferior premotor regions and the genu contains fibers from the prefrontal regions (25). Thus, our findings of significantly decreased FA with increased MD values in the rostrum and genu in Group A to those in the controls can be attributed to microstructural changes secondary to injury in the frontal lobe.

In this study, Group B patients had circumscribed lesions in the temporo-occipital lobes. The callosal fibers originating from the occipital and temporal lobes constitute the isthmus and splenium of the CC (25). Decreased FA along with increased MD in both the isthmus and splenium of Group B patients can be attributed to circumscribed lesions in the occipito-temporal lobes. Group C patients, had circumscribed lesions in the frontal, parietal, and temporal lobes, and showed decreased FA along with increased MD in all the subdivisions of the CC. Thus, in contrast to Group A and B patients, Group C patients also showed microstructural damage in the RB, AMB, and PMB subdivisions of the CC. It has been documented that fibers from the RB and AMB course through the premotor/supplementary motor areas and motor somesthetic areas, respectively (25). Fibers from the posterior parietal regions constitute the PMB (25). We speculate that the microstructural damage observed in the anterior callosal subdivisions (rostrum, genu, and RB), AMB, and PMB is a consequence of the primary lesion sites being in the fronto-parietal lobes in Group C patients.

The findings of the present study correspond with previous studies that have reported reduced FA and increased MD in sites of secondary degeneration (52, 53). Additional studies have established temporal alterations in MD values in subjects with TBI (16, 54), whereby MD initially decreases due to cytotoxic edema and later normalizes or elevates as result of either recovery or gliosis during the WD process. This indicates that the timing of imaging post-injury is a crucial factor in determining diffusivity changes. In Group C, though a few (RB, AMB, PMB, and Isthmus) showed a trend towards an increase. This may be attributed to the wide range in the time interval between injury and image acquisition, which ranged from 14 days (sub-acute) to 6 months (chronic) post-injury in the patients with TBI.

The limitations of our study were the small number of patients and wide variation in the time interval between image acquisition and injury within the TBI patient groups. In conclusion, this study describes the cortico-callosal topographical relationship in patients with TBI. We observed a decline in FA and increase in MD values that appeared to represent regional WD. These findings may contribute to our understanding of why patients with the same severity of TBI present with a wide variation of deficits in cognitive functions.

Acknowledgements

The authors would like to thank the participants of the study. This work was done as R&D project INM-311supported from defence research and development organization (DRDO), India. Miss. Kavita Singh would like to acknowledge the fellowship grant from Department of Science and Technology (DST), New Delhi, India.

Authors' Contributions

1: Guarantor of integrity of the entire study: Dr Richa Trivedi; 2: Study concepts: Dr Richa Trivedi; 3: Study design: Dr Richa Trivedi, Ms Kavita Singh; 4: Definition of intellectual content: Dr Richa Trivedi, Ms Kavita Singh; 5: Literature research: Ms Kavita Singh; 6: Clinical studies: Ms Kavita Singh, Dr Maria, Dr Ajay Chaudhary, Dr Rajendra P. Tripathi; 7: Experimental studies: NA; 8: Data acquisition: Ms Kavita Singh, Mr Pawan Kumar; 9: Data analysis: Ms Kavita Singh, Dr Richa Trivedi, Dr Maria M. D'souza, Dr Ajay Chaudhary; 10: Statistical analyses: Ms Kavita Singh; 11: Manuscript preparations: Ms Kavita Singh; 12: Manuscript editing: Dr Richa Trivedi, Dr Subash Khushu; 13: Manuscript review: Dr Rajendra P. Tripathi The authors would like to thank the participants of the study. Ms. Kavita Singh would like to acknowledge the fellowship grant from department of science and technology (DST), New Delhi, India.

References

1. Menon DK, Schwab K, Wright DW, Maas AI. Position Statement: Definition of Traumatic Brain Injury. *Arch Phys Med Rehabil.* 2010;**91**(11):1637–40.
2. Vandromme M, Melton SM, Kerby JD. Progesterone in traumatic brain injury: time to move on to phase III trials. *Crit Care.* 2008;**12**(3):153.
3. Levin HS. Neurobehavioral outcome of closed head injury: implications for clinical trials. *J Neurotrauma.* 1995;**12**(4):601–10.
4. Junque C. [Neuropsychological sequelae of head injury]. *Rev Neurol.* 1999;**28**(4):423–9.
5. Salmond CH, Menon DK, Chatfield DA, Williams GB, Pena A, Sahakian BJ, et al. Diffusion tensor imaging in chronic head injury survivors: correlations with learning and memory indices. *Neuroimage.* 2006;**29**(1):117–24.
6. Povlishock JT, Christman CW. The Pathobiology of Traumatically Induced Axonal Injury in Animals and Humans: A Review of Current Thoughts. *J Neurotrauma.* 1995;**12**(4):555–64.
7. Oni MB, Wilde EA, Bigler ED, McCauley SR, Wu TC, Yallampalli R, et al. Diffusion tensor imaging analysis of frontal lobes in pediatric traumatic brain injury. *J Child Neurol.* 2010;**25**(8):976–84.
8. Buki A, Povlishock JT. All roads lead to disconnection?–Traumatic axonal injury revisited. *Acta Neurochir (Wien).* 2006;**148**(2):181–93.
9. Arfanakis K, Haughton VM, Carew JD, Rogers BP, Dempsey RJ, Meyerand ME. Diffusion tensor MR imaging in diffuse axonal injury. *AJNR Am J Neuroradiol.* 2002;**23**(5):794–802.
10. Mori S, Zhang J. Principles of diffusion tensor imaging and its applications to basic neuroscience research. *Neuron.* 2006;**51**(5):527–39.
11. Chanraud S, Zahr N, Sullivan EV, Pfefferbaum A. MR diffusion tensor imaging: a window into white matter integrity of the working brain. *Neuropsychol Rev.* 2010;**20**(2):209–25.
12. Madden DJ, Bennett IJ, Song AW. Cerebral White Matter Integrity and Cognitive Aging: Contributions from Diffusion Tensor Imaging. *Neuropsychol Rev.* 2009;**19**:415–35.
13. Wu TC, Wilde EA, Bigler ED, Li X, Merkley TL, Yallampalli R, et al. Longitudinal changes in the corpus callosum following pediatric traumatic brain injury. *Dev Neurosci.* 2010;**32**(5-6):361–73.
14. Babikian T, Prins ML, Cai Y, Barkhoudarian G, Hartonian I, Hovda DA, et al. Molecular and physiological responses to juvenile traumatic brain injury: focus on growth and metabolism. *Dev Neurosci.* 2010;**32**(5-6):431–41.
15. Bendlin BB, Ries ML, Lazar M, Alexander AL, Dempsey RJ, Rowley HA, et al. Longitudinal changes in patients with traumatic brain injury assessed with diffusion-tensor and volumetric imaging. *Neuroimage.* 2008;**42**(2):503–14.
16. Huisman TA, Schwamm LH, Schaefer PW, Koroshetz WJ, Shetty-Alva N, Ozsunar Y, et al. Diffusion tensor imaging as potential biomarker of white matter injury in diffuse axonal injury. *AJNR Am J Neuroradiol.* 2004;**25**(3):370–6.
17. Inglese M, Makani S, Johnson G, Cohen BA, Silver JA, Gonen O, et al. Diffuse axonal injury in mild traumatic brain injury: a diffusion tensor imaging study. *J Neurosurg.* 2005;**103**(2):298–303.
18. Kumar R, Saksena S, Husain M, Srivastava A, Rathore RK, Agarwal S, et al. Serial changes in diffusion tensor imaging metrics of corpus callosum in moderate traumatic brain injury patients and their correlation with neuropsychometric tests: a 2-year follow-up study. *J Head Trauma Rehabil.* 2010;**25**(1):31–42.
19. Levin HS, Wilde EA, Chu Z, Yallampalli R, Hanten GR, Li X, et al. Diffusion tensor imaging in relation to cognitive and functional outcome of traumatic brain injury in children. *J Head Trauma Rehabil.* 2008;**23**(4):197–208.
20. Little DM, Kraus MF, Joseph J, Geary EK, Susmaras T, Zhou XJ, et al. Thalamic integrity underlies executive dysfunction in traumatic brain injury. *Neurology.* 2010;**74**(7):558–64.
21. Nakayama N, Okumura A, Shinoda J, Yasokawa YT, Miwa K, Yoshimura SI, et al. Evidence for white matter disruption in traumatic brain injury without macroscopic lesions. *J Neurol Neurosurg Psychiatry.* 2006;**77**(7):850–5.
22. Beauchamp MH, Anderson VA, Catroppa C, Maller JJ, Godfrey C, Rosenfeld JV, et al. Implications of reduced callosal area for social skills after severe traumatic brain injury in children. *J Neurotrauma.* 2009;**26**(10):1645–54.
23. Ewing-Cobbs L, Prasad MR, Swank P, Kramer L, Cox CJ, Fletcher JM, et al. Arrested development and disrupted callosal microstructure following pediatric traumatic brain injury: relation to neurobehavioral outcomes. *Neuroimage.* 2008;**42**(4):1305–15.
24. Banich MT. *Interhemispheric interaction: Mechanisms of unified processing.* New Jersey: Hillsdale; 1995.
25. Witelson SF. Hand and sex differences in the isthmus and genu of the human corpus callosum. A postmortem morphological study. *Brain.* 1989;**112 (Pt 3)**:799–835.
26. Galaburda AM, Sherman GF, Rosen GD, Aboitiz F, Geschwind N. Developmental dyslexia: four consecutive patients with cortical anomalies. *Ann Neurol.* 1985;**18**(2):222–33.
27. Keary CJ, Minshew NJ, Bansal R, Goradia D, Fedorov S, Keshavan MS, et al. Corpus callosum volume and neurocognition in autism. *J Autism Dev Disord.* 2009;**39**(6):834–41.
28. Lee SY, Kim SS, Kim CH, Park SW, Park JH, Yeo M. Prediction of outcome after traumatic brain injury using clinical and neuroimaging variables. *J Clin Neurol.* 2012;**8**(3):224–9.
29. Hughes DG, Jackson A, Mason DL, Berry E, Hollis S, Yates DW. Abnormalities on magnetic resonance imaging seen acutely following mild traumatic brain injury: correlation with neuropsychological tests and delayed recovery. *Neuroradiology.* 2004;**46**(7):550–8.
30. Guskiewicz KM, Marshall SW, Bailes J, McCrea M, Cantu RC, Randolph C, et al. Association between recurrent concussion and late-life cognitive impairment in retired professional football players. *Neurosurgery.* 2005;**57**(4):719–26.
31. Mathias JL, Bigler ED, Jones NR, Bowden SC, Barrett-Woodbridge M, Brown GC, et al. Neuropsychological and information processing performance and its relationship to white matter changes following moderate and severe traumatic brain injury: a preliminary study. *Appl Neuropsychol.* 2004;**11**(3):134–52.
32. Mao H, Zhang L, Yang KH, King AI. Application of a finite element model of the brain to study traumatic brain injury mechanisms in the rat. *Stapp Car Crash J.* 2006;**50**:583–600.
33. Teasdale G, Jennett B. Assessment of coma and impaired consciousness. A practical scale. *Lancet.* 1974;**2**(7872):81–4.

34. Rathore RK, Gupta RK, Agarwal S, Trivedi R, Tripathi RP, Awasthi R. Principal eigenvector field segmentation for reproducible diffusion tensor tractography of white matter structures. *Magn Reson Imaging.* 2011;**29**(8):1088–100.
35. Jiang H, van Zijl PC, Kim J, Pearlson GD, Mori S. DtiStudio: resource program for diffusion tensor computation and fiber bundle tracking. *Comput Methods Programs Biomed.* 2006;**81**(2):106–16.
36. Kampfl A, Franz G, Aichner F, Pfausler B, Haring HP, Felber S, et al. The persistent vegetative state after closed head injury: clinical and magnetic resonance imaging findings in 42 patients. *J Neurosurg.* 1998;**88**(5):809–16.
37. Mac Donald CL, Dikranian K, Bayly P, Holtzman D, Brody D. Diffusion tensor imaging reliably detects experimental traumatic axonal injury and indicates approximate time of injury. *J Neurosci.* 2007;**27**(44):11869–76.
38. Parizel PM, Van Goethem JW, van den Hauwe L, Dillen C, Verlooy J, Ozsarlak. et al. Imaging findings in diffuse axonal injury after closed head trauma. *Eur Radiol.* 1998;**8**(6):960–5.
39. Bigler ED. Traumatic brain injury, neuroimaging, and neurodegeneration. *Front Hum Neurosci.* 2013;**7**:395.
40. Waller A. Experiments on the Section of the Glossopharyngeal and Hypoglossal Nerves of the Frog, and Observations of the Alterations Produced Thereby in the Structure of Their Primitive Fibres. *Philos Trans R Soc Lond.* 1850;**140**:423–9.
41. Wang JT, Medress ZA, Barres BA. Axon degeneration: molecular mechanisms of a self-destruction pathway. *J Cell Biol.* 2012;**196**(1):7–18.
42. Graham DI, Genarrelli TA, McIntosh TK. Trauma . In: Graham DI, Lantos PL, editors. *Greenfield's Neuropathology.* London: Arnold Publishers; 2002. pp. 823–98.
43. Griffin JW, George EB, Hsiesh ST, Glass JD. Axonal degeneration and disorders of the axonal cytoskeleton. In: Waxman SG, Kocsis JD, Sytys PK editors. *The Axon: Structure, Function and Pathophysiology.* New York: Oxford University Press; 1995. pp. 3750–90.
44. Vargas ME, Barres BA. Why is Wallerian degeneration in the CNS so slow? *Annu Rev Neurosci.* 2007;**30**:153–79.
45. Kuhn MJ, Johnson KA, Davis KR. Wallerian degeneration: evaluation with MR imaging. *Radiology.* 1988;**168**(1):199–202.
46. Yu C, Zhu C, Zhang Y, Chen H, Qin W, Wang M, et al. A longitudinal diffusion tensor imaging study on Wallerian degeneration of corticospinal tract after motor pathway stroke. *Neuroimage.* 2009;**47**(2):451–8.
47. Pierpaoli C, Barnett A, Pajevic S, Chen R, Penix LR, Virta A, et al. Water diffusion changes in Wallerian degeneration and their dependence on white matter architecture. *Neuroimage.* 2001;**13**(6 Pt 1):1174–85.
48. Saksena S, Jain R, Schultz L, Jiang Q , Soltanian-Zadeh H, Scarpace L, et al. The Corpus Callosum Wallerian Degeneration in the Unilateral Brain Tumors: Evaluation with Diffusion Tensor Imaging (DTI). *J Clin Diagn Res.* 2013;**7**(2):320–5.
49. Kim H, Piao Z, Liu P, Bingaman W, Diehl B. Secondary white matter degeneration of the corpus callosum in patients with intractable temporal lobe epilepsy: a diffusion tensor imaging study. *Epilepsy Res.* 2008;**81**(2-3):136–42.
50. Pandya DN, Karol EA, Heilbronn D. The topographical distribution of interhemispheric projections in the corpus callosum of the rhesus monkey. *Brain Res.* 1971;**32**(1):31–43.
51. de Lacoste MC, Kirkpatrick JB, Ross ED. Topography of the human corpus callosum. *J Neuropathol Exp Neurol.* 1985;**44**(6):578–91.
52. Brandstack N, Kurki T, Hiekkanen H, Tenovuo O. Diffusivity of normal-appearing tissue in acute traumatic brain injury. *Clin Neuroradiol.* 2011;**21**(2):75–82.
53. Matsushita M, Hosoda K, Naitoh Y, Yamashita H, Kohmura E. Utility of diffusion tensor imaging in the acute stage of mild to moderate traumatic brain injury for detecting white matter lesions and predicting long-term cognitive function in adults. *J Neurosurg.* 2011;**115**(1):130–9.
54. Ito J, Marmarou A, Barzo P, Fatouros P, Corwin F. Characterization of edema by diffusion-weighted imaging in experimental traumatic brain injury. *J Neurosurg.* 1996;**84**(1):97–103.